

Inductive Bias-driven Reinforcement Learning For Efficient Schedules in Heterogeneous Clusters

Subho S. Banerjee¹, Saurabh Jha¹, Ravishankar K. Iyer^{1,2}

¹Department of Computer Science, ²Department of Electrical and Computer Engineering
University of Illinois at Urbana-Champaign
Urbana, IL 61801

Abstract

The problem of scheduling of workloads onto heterogeneous processors (e.g., CPUs, GPUs, FPGAs) is of fundamental importance in modern datacenters. Most current approaches rely on building application/system-specific heuristics that have to be reinvented on a case-by-case basis. This can be prohibitively expensive and is untenable going forward. In this paper, we propose a domain-driven reinforcement learning (RL) model for scheduling that can be broadly applied to a large class of heterogeneous processors. The key novelty of our approach is (i) the RL model; and (ii) the significant reduction of training-data (using domain knowledge) and -time (using sampling based end-to-end gradient propagation). We demonstrate the approach using real world GPU and FPGA accelerated applications to produce scheduling policies that significantly outperform hand-tuned heuristics.

1 Introduction

The problem of scheduling of workloads on heterogeneous processing fabrics (e.g., GPUs, FPGAs, which are becoming the norm in datacenters [1, 2]), is at its core an intractable NP-hard problem [3, 4]. The current scheduling approaches rely on application- and system-specific heuristics with extensive domain-expert driven tuning of scheduling policies which have to be reinvented on a case-by-case basis (e.g., [5–17]). This is a fundamental challenge, as variation across (i) workloads, (ii) deployments across datacenter vendors, and (iii) machine configurations inside a datacenter lead to significant time and money is spent in painstakingly building scheduling heuristics.

In this paper, we address this issue by formulating the problem of scheduling of workloads on to a processing fabric as a partially observable Markov decision process (POMDP) [18, 19] which can automatically and rapidly train efficient scheduling policies without human intervention. Specifically, we use a domain guided Bayesian model-based POMDP to decrease the amount of training data (i.e., sampled trajectories), and sampling of the Bayesian model so as to reduce the end-to-end training time for the POMDP. Hence, significantly reducing the cost of (i) running a large heterogeneous computing system using an efficient scheduling policy; and (ii) training the policy itself.

Reducing Training Data. State of the art methods for choosing an optimal action in POMDPs rely on training neural networks (NNs) [20, 21]. As these approaches are model-free, training the NN requires large quantities of data and time to compute meaningful policies. In contrast, we provide an inductive bias to the reinforcement learning (RL) agent by encoding domain knowledge as a Bayesian model to infer the latent state from observations, while at the same time leveraging the scalability of deep learning methods through end-to-end gradient descent. In the case of scheduling, this inductive bias is a set of statistical relationships between measurements from microarchitectural monitors [22]. To the best of our knowledge, this is the first paper to exploit these relationships and measurements to infer resource utilization in the system (i.e., latent state) to build RL-based scheduling policies.

Reducing Training Time. The addition of the inductive bias while making the training process less data hungry (i.e., less number of workload executions to train the model), comes at the cost of additional training time – the cost of performing full-Bayesian inference at every training step [23–25].

Preprint. Under review.

It is this cost that makes the use of deep RL techniques in dynamic real-world deployments (which require periodic retraining) prohibitively expensive. To address this issue, we develop a procedure to compute the gradient of variables in the above Bayesian model without requiring full inference computation (in contrast to prior work [24, 25]). The key is to calculate the gradient by generating samples from the model, which is computationally simpler than inferring the posterior distribution.

The remainder of the paper discusses the major contributions in this work. (i) The sampling based training technique in the context of general POMDPs (in §2 and §3). (ii) The particular POMDP formulation to solve heterogeneous scheduling problem (in §4). (iii) The evaluation of the scheduling strategy on several real-world GPU and FPGA accelerated workloads (in §5). The proposed framework drastically reduces the average job completion time over hand-tuned scheduling heuristics by as much as 32%, and to within 6% of an oracle scheduler with training time improvement of 4 \times compared to full Bayesian inference based on belief propagation. We believe that the proposed approach is representative of RL applied to several problems relating to the control of engineered systems (e.g., industrial scheduling, datacenter network scheduling) where data-driven approaches can be augmented with domain knowledge to build sample efficient algorithms to train RL agents.

2 Background

Partially Observable Markov Decision Processes. A POMDP is a stochastic model describing relationships between an agent and its environment. It is a tuple $(\mathcal{S}, \mathcal{A}, \mathcal{T}, \Omega, O, R, \gamma)$, where \mathcal{S} is the state space, \mathcal{A} is the action space, and Ω is the observation space. We denote $s_t \in \mathcal{S}$ as the hidden state at time t . When an action $a_t \in \mathcal{A}$ is executed, the state changes according to the transition distribution, $s_{t+1} \sim \mathcal{T}(s_{t+1}|s_t, a_t)$. Subsequently, the agent receives a noisy or partially occluded observation $o_{t+1} \in \Omega$ according to the distribution $o_{t+1} \sim O(o_{t+1}|s_{t+1}, a_t)$, and a reward $r_{t+1} \in \mathbb{R}$ according to the distribution $r_{t+1} \sim R(r_{t+1}|s_{t+1}, a_t)$.

An agent acts according to its policy $\pi(a_t|s_t)$ which returns the probability of taking action a_t at time t . The agent’s goal is to learn a policy π that maximises the expected future reward $J = \mathbb{E}_{\tau \sim p(\tau)} [\sum_{t=1}^T \gamma^{t-1} r_t]$ over trajectories $\tau = (s_0, a_0, \dots, a_{T-1}, s_T)$ induced by its policy, where $\gamma \in [0, 1)$ is the discount factor. In general, a POMDP agent must infer the belief state $b_t = \Pr(s_t|o_1, \dots, o_t, a_0, \dots, a_{t-1})$, which is used to calculate $\pi(a_t|\hat{s}_t)$ where $\hat{s}_t \sim b_t$. In the remainder of the paper we will use $\pi(a_t|\hat{s}_t)$ and $\pi(a_t|b_t)$ interchangeably.

Related Work. Finding solutions for many POMDPs involves (i) estimating the transition model T and observation model O , (ii) performing inference under this model, and (iii) choosing an action based on the inferred belief state. Prior work in this area has extensively explored the use of NNs, particularly recurrent NNs (RNNs) as universal function approximators for (i) and (iii) above because of their ease in training and inference (e.g., [26–32]). Neural networks have proven to be extremely effective at learning but usually require a lot of data (in this case, sampled trajectories, which may be prohibitively expensive to acquire for certain class of applications such as scheduling). The ability to incorporate explicit domain knowledge (in the case of scheduling which is based on system design invariants) could significantly reduce the amount of data required. To this end, other work [31, 33, 34] has advocated the integration of probabilistic models (including Bayesian filter models) for (i) above. The significant computational cost of learning and inference in these models have spurred the use of approximation techniques for training and inference, including NN based approximations of Bayesian inference [31, 32] and variational inference methods [34].

In this paper, we too advocate the use of a domain-driven probabilistic model for b_t and which can be trained through end-to-end backpropagation to compute a policy. Specifically, the technique handles the case of performing gradient descent on a Bayesian network (BN) with known structure and incomplete observations without performing inference on the BN, only requiring generation of samples from the model. This is contrary to prior work on learning BNs using gradient descent [24, 25] or expectation maximization, both of which require full posterior inference at every training step.

Actor-Critic Methods. Actor-Critic methods [35] have been previously proposed to learn the parameters ρ of an agent’s policy $\pi_\rho(a_t|s_t)$. Here (i) the “Critic” estimates the value function $V(s)$; and (ii) the “Actor” updates the policy distribution $\pi(a|s)$ in the direction suggested by the Critic. In this paper, we use n -step learning with asynchronous advantage actor-critic (A3C) and its synchronous simplification, the advantage actor-critic (A2C) method [20].

For n -step learning, starting at time t , the current policy performs n_s consecutive steps in n_e parallel environments. The gradient update of π and V are based on this mini-batch of size $n_e n_s$. The target

for the value-function $V_\eta(s_{t+i})$, $i \in [0, n_s]$, parameterized by η , is the appropriately discounted sum of on-policy rewards up until $t + n_s$ and the off-policy bootstrapped value $V_\eta^*(s_{t+n_s})$. Using an advantage function $A_\eta^{t,i} = (\sum_{j=0}^{n_s-i-1} \gamma^j r_{t+i+j}) + \gamma^{n_s-i} V_\eta^*(s_{t+n_s}) - V_\eta(s_{t+1})$, the A2C loss for the policy parameters ρ , the value function loss for parameters η are

$$\mathcal{L}_t^A(\rho) = -\frac{1}{n_e n_s} \sum_{e=0}^{n_e-1} \sum_{i=0}^{n_s-1} \mathbb{E}_{s_{t+i} \sim b_{t+i}} [\log \pi_\rho(a_{t+i}|s_{t+i}) A_\eta^{t,i}(s_{t+i}, a_{t+i})] \quad (1a)$$

$$\mathcal{L}_t^V(\eta) = \frac{1}{n_e n_s} \sum_{e=0}^{n_e-1} \sum_{i=0}^{n_s-1} \mathbb{E}_{s_{t+i} \sim b_{t+i}} [A_\eta^{t,i}(s_{t+i}, a_{t+i})^2]. \quad (1b)$$

3 Training POMDP RL-Agent with Backpropagation

We consider a special case of the POMDP formulation presented above (illustrated in Fig. 1). We assume that the domain knowledge about the environment of the RL-agent is presented as a joint probability distribution $\Pr(s_t, a_{t-1}, o_t; \Theta_{BN})$ that can be factorized as a BN (with parameters Θ_{BN}). A BN is a probabilistic graphical model that represents a set of variables and their conditional dependencies via a directed acyclic graph (DAG). We use probabilistic inference on the BN to calculate an estimate of the belief state \hat{b}_t . \hat{b}_t is then used in with a NN $f_\pi(\hat{b}_t; \Theta_\pi)$ (with parameters Θ_π) to approximate RL-agent's policy, and a NN $f_V(\hat{b}_t; \Theta_V)$ (with parameters Θ_V) to approximate the state based value function. We refer to all the parameters of the model as $\Theta = (\Theta_{BN}, \Theta_\pi, \Theta_V) = (\rho, \eta)$. The model is then trained by propagating the gradient of the total loss $\nabla_{\Theta} \mathcal{L}_t^{RL} = \nabla_{\Theta} \mathcal{L}_t^A(\rho) + \nabla_{\Theta} \mathcal{L}_t^V(\eta)$. Estimating this gradient requires us to compute $\nabla_{\Theta_{BN}} \hat{b}_t$. Traditional methods for computing this gradient require inference computation [24, 25]. However, even approximate inference in such models is known to be NP-Hard [23]. Below we describe an algorithm to approximate the gradient without requiring computation of full Bayesian inference. All that is required is the ability to generate samples from the BN. Only the subset of the BN necessary for generation of the samples is expanded. These samples are then used as a representation of the distribution of the BN. As a result, the proposed method decouples the training of the BN from the inference procedure used on it to calculate \hat{b}_t .

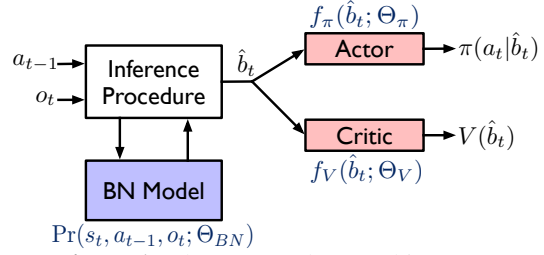


Figure 1: The proposed RL architecture.

3.1 The Bayesian Network & Its Gradient

Let the BN described above be a DAG (V, E) , and let $\mathbf{X} = \{X_v | v \in V\}$ be a set of random variables indexed by V . Associated with each node X is a conditional probability density function $\Pr(X|\varphi(X))$, where $\varphi(X)$ are the parents of X in the graph. We assume that we are given (i) an efficient algorithm to sample values of X given $\varphi(X)$, and (ii) a function $f_X(x, y; \theta_X) = \Pr_{\theta_X}(X = x | \varphi(X) = y)$ whose partial derivative with respect to θ_X is known and efficiently computable. The BN can also have deterministic relationships between two random variables, under the assumption that the relationship is a differentiable diffeomorphism. That is, for random variables X, Y , and diffeomorphism F , $\Pr(Y = y) = \Pr(X = F^{-1}(y)) |DF^{-1}(y)|$ where DF^{-1} is the inverse of the Jacobian of F .

Computing Gradient. For a random variable X in the BN, its parents $\varphi(X)$, its ancestor set $\Xi(X) = \{Y | Y \rightsquigarrow X \wedge Y \notin \varphi(X)\}$ (where \rightsquigarrow represents a directed path in the BN). We now define a procedure to approximately compute the gradient of X with respect to Θ_{BN} . We do this in two parts: (i) $\partial \Pr(X=x|\xi=\mathbf{a})/\partial \theta_X$ and (ii) $\nabla_{\Theta_{BN} \setminus \theta_X} \Pr(X=x|\xi=\mathbf{a})$ for $\xi \subseteq \Xi(X)$. First,

$$\begin{aligned} \frac{\partial \Pr(X=x|\xi=\mathbf{a})}{\partial \theta_X} &= \frac{\partial}{\partial \theta_X} \int \Pr(\varphi(X) = \mathbf{y} | \xi = \mathbf{a}) \Pr(X=x | \varphi(X) = \mathbf{y}, \xi = \mathbf{a}) d\mathbf{y} \\ &= \frac{\partial}{\partial \theta_X} \int \Pr(\varphi(X) = \mathbf{y} | \xi = \mathbf{a}) f_X(x, \mathbf{y}; \theta_X) d\mathbf{y} = \int \Pr(\varphi(X) = \mathbf{y} | \xi = \mathbf{a}) \frac{\partial f_X(x, \mathbf{y}; \theta_X)}{\partial \theta_X} d\mathbf{y} \end{aligned}$$

$$\approx \sum_{i=1}^S \frac{n_S(\mathbf{a}, \mathbf{y}_i)}{n_S(\mathbf{a})} \frac{\partial f_X(x, \mathbf{y}_i; \theta_X)}{\partial \theta_X}. \quad (2)$$

Here S samples are drawn from a variable(s) Z such that $n_S(j)$ is the number of times the value j appears in the set of samples $\{z_i\}$, i.e., $n_S(j) = \sum_{i=1}^S \mathbb{1}\{z_i = j\}$. Next,

$$\begin{aligned} \nabla_{\Theta_{BN \setminus \theta_X}} \Pr(X = x | \xi = \mathbf{a}) &= \nabla_{\Theta_{BN \setminus \theta_X}} \int \Pr(\wp(X) = \mathbf{y} | \xi = \mathbf{a}) \Pr(X = x | \wp(X) = \mathbf{y}, \xi = \mathbf{a}) d\mathbf{y} \\ &= \int f_X(x, \mathbf{y}; \theta_X) \nabla_{\Theta_{BN \setminus \theta_X}} \Pr(\wp(X) = \mathbf{y} | \xi = \mathbf{a}) d\mathbf{y} \\ &\approx \sum_{i=1}^S \frac{n_S(\mathbf{y}_i)}{S} f_X(x, \mathbf{y}_i; \theta_X) \nabla_{\Theta_{BN \setminus \theta_X}} \Pr(\wp(X) = \mathbf{y}_i | \xi = \mathbf{a}) \end{aligned} \quad (3)$$

In the case that $|\wp(X)| > 1$, variables in $\wp(X)$ might not be conditionally independent given $\Xi(X)$. Hence we need to find a set of nodes N such that $I \perp J | \Xi(X) \cup N \forall I, J \in \wp(X)$. Now,

$$\begin{aligned} \Pr(\wp(X) = \mathbf{y}_i | \xi = \mathbf{a}) &= \int \Pr(N = \mathbf{n} | \xi = \mathbf{a}) \Pr(\wp(X) = \mathbf{y} | N = \mathbf{n}, \xi = \mathbf{a}) d\mathbf{n} \\ &= \int \Pr(N = \mathbf{n} | \xi = \mathbf{a}) \prod_{j=1}^m \Pr(P_j = y_j | N = \mathbf{n}, \xi = \mathbf{a}) d\mathbf{n} \\ &\approx \sum_{k=1}^S \frac{n_S(\mathbf{a}, \mathbf{n}_k)}{n_S(\mathbf{a})} \prod_{j=1}^m \Pr(P_j = y_j | N = \mathbf{n}_k, \xi = \mathbf{a}), \end{aligned} \quad (4)$$

where $\wp(X) = (P_1, \dots, P_m)$ and $\mathbf{y}_i = (y_{i,1}, \dots, y_{i,m})$. So, we have,

$$\begin{aligned} \nabla_{\Theta_{BN \setminus \theta_X}} \Pr(\wp(X) = \mathbf{y}_i | \xi = \mathbf{a}) &\approx \sum_{k=1}^S \frac{n_S(\mathbf{a}, \mathbf{n}_k)}{n_S(\mathbf{a})} \nabla_{\Theta_{BN \setminus \theta_X}} \prod_{j=1}^m \Pr(P_j = y_{i,j} | N = \mathbf{n}_k, \xi = \mathbf{a}) \\ &= \sum_{k=1}^S \frac{n_S(\mathbf{a}, \mathbf{n}_k)}{n_S(\mathbf{a})} \sum_{l=1}^m \left(\prod_{h=1, h \neq l}^m \Pr(P_h = y_{i,h} | N = \mathbf{n}_k, \xi = \mathbf{a}) \right) \nabla_{\Theta_{BN \setminus \theta_X}} \Pr(P_l = y_{i,l} | N = \mathbf{n}_k, \xi = \mathbf{a}) \\ &\approx \sum_{k=1}^S \frac{n_S(\mathbf{a}, \mathbf{n}_k)}{n_S(\mathbf{a})} \sum_{l=1}^m \left(\prod_{h=1, h \neq l}^m \frac{n_S(y_{i,h}, \mathbf{a}, \mathbf{n}_k)}{n_S(\mathbf{a}, \mathbf{n}_k)} \right) \overbrace{\nabla_{\Theta_{BN \setminus \theta_X}} \Pr(P_l = y_{i,l} | N = \mathbf{n}_k, \xi = \mathbf{a})}^{\text{Expand by recursion using Eqns. 2, 3 and 5}}. \end{aligned} \quad (5)$$

Using Eqns. 2, 3 and 5, we can now recursively calculate the gradient of the conditional probability density of any variable given the value of it's ancestors, thereby calculating $\nabla_{\Theta_{BN}} \hat{b}_t$.

Computational Complexity. The cost of computing Eqns. 2 and 3 is $O(S)$. The cost of computing Eqn. (5) is $O(mS)$. The cost of finding N is $O(|\wp(s_t)|^2(|V| + |E|))$ (i.e., running the Bayes ball algorithm [36] for every pair of nodes in $\wp(X)$). The total computational complexity of the entire procedure hinges on finding the number of times the Eqns. 2, 4 and 5 are executed, which we refer to as Q . Q depends on the size of N and on the graphical structure of the BN. Hence, the total cost of computing $\nabla_{\Theta_{BN}} \hat{b}_t$ is $O(Q(|\wp(s_t)|^2(|V| + |E|) + mS))$ (where $|\wp(s_t)| \leq |V| - 1$), and this is computed $n_s n_e |b_t|$ times during training. Note that for a polytree BN (the structure of the BN we will use in the §4), $N = \emptyset$, and $Q \leq |V|$. This is still better than belief propagation on the polytree with the gradient computation technique from [24, 25], which is $O(|V| \max_{v \in V} (dom(X_v)))$, where $dom(X)$ is the size of the domain of X , which in our case could be exponentially large.

4 Scheduling Datacenter Workloads Using Reinforcement Learning

We now demonstrate an application of the POMDP model and training methodology presented in §3 to the problem of scheduling tasks to a heterogeneous processing fabric including CPUs, GPUs and FPGAs. The model integrates real-time performance measurements, prior knowledge about

workloads, and system architecture to (i) dynamically infer system state (i.e., resource utilization), and (ii) automatically schedule tasks to a heterogeneous processing fabric.

Workload & Programming Model. The system workload consists of multiple user programs where each program is expressed as a *data flow graph* (DFG), a DAG representing the input-output relationships between operations (which we refer to as *kernels*). Prior work has shown that a large number of applications can be expressed as compositions of such kernels [37, 38]. A prominent examples of such composition are modern data analytics and machine learning (ML) frameworks that describe workloads as DFGs [39–42]. We assume that these kernels are known ahead of time and have multiple implementations available for different processors and accelerators. Once trained, our approach can schedule any composition (DFG) of these kernels, but requires retraining when the set of available kernels are changed. The key challenges that arises in this setting are

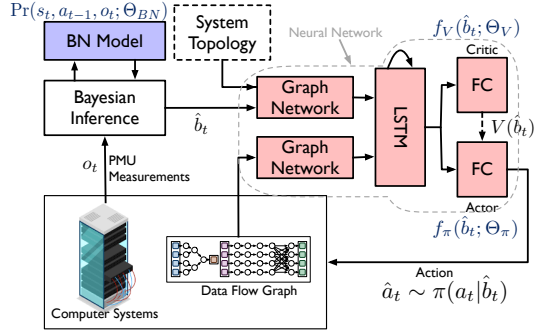


Figure 2: Architecture of the scheduling model.

hides others from direct measurement (e.g., amount of memory bandwidth used by a CPU). We use real-time performance counter [22] measurements (o_t) to infer the utilization of these “hidden” resources. Performance counters (PC) are special purpose registers present in the CPU and other accelerators for characterization of an applications’ behavior and identification of microarchitectural performance bottlenecks. Specifically, we use a BN to (i) model aleatoric uncertainty in these measurements, and (ii) encode our knowledge about system architecture in terms of invariants or statistical relationships between the measurements. Inference on this BN then gives us an accurate estimate of the latent state of the system. Second, we use a RNN (i.e., $f_\pi(\cdot)$ and $f_V(\cdot)$) to learn scheduling policies for user programs that minimize resource contention and maximize performance. These two ML models, effectively decouple system architecture- and measurement-specific aspects of scheduling (the BN) from its optimization aspects (the NN). The compelling value of the above architecture (and its two constituent models) is that it can automatically generate scheduling policies for the deployment of accelerator-centric DFG in both truly heterogeneous and dynamically changing multi-tenant environments (like clouds) all without requiring configuration specific, and painstakingly tuned heuristics like state of the art. This improves overall performance, resource utilization, and enables fine-grained resource sharing across workloads.

Performance Counters. The PCs are generally relied upon to conduct low-level performance analysis or tuning of performance bottlenecks in applications. As the source of these bottlenecks are generally the unavailability of system resources, the performance counter can naturally be used to estimate resource utilization of a system. Another benefit of using PCs is that no source code modifications is needed in the application to make measurements. The PCs can be grouped into three categories, (i) those pertaining to the processing fabric (CPU core or accelerators), (ii) those pertaining to the memory subsystem, and (iii) those pertaining to the system interconnect (in our case PCIe). Fig. 3 illustrates an organization of a computer system as well as the categories above. As the CPU orchestrates all execution in the computer (even for accelerators), we find that it is sufficient to make PC measurements on the CPU to ascertain the current utilization of almost all system resources (i.e., those that matter for scheduling).

BN Model. The measurements made from performance counters have some inherent noise [43]. (i) The measurements can only be stored in a fixed number of registers. Hence only a fixed number of measurements can be made at one point in time. As a result, successive measurements have to be made, which capture marginally different system state. (ii) Particular performance counters might become unavailable (or return incorrect values). (iii) In the case that a single scheduling agent is controlling a cluster of machines (which is the common case in datacenters), measurements made on different machines are not in sync and are often delayed by network latency. As a result, PCs are often

(i) how should one select between the above implementations of kernels, and (ii) where to run them when executing an application.

POMDP Architecture. The overall architecture of the proposed POMDP model is illustrated in Fig. 2. The first part of the POMDP models the latent state \hat{b}_t of the computer system. For the scheduling problem, this corresponds to resource utilization of various components of the computer system. Utilization of some of these resource can be measured directly in software (e.g., amount of free memory), however, the different layers of abstraction of the computer stack

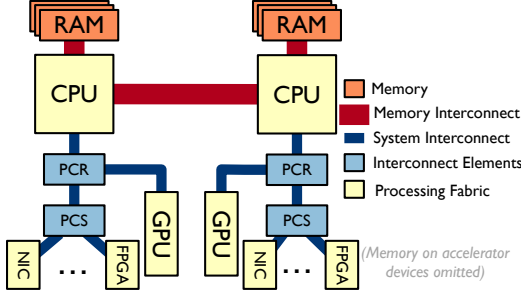


Figure 3: Organization of a multi-CPU computer. (PCR = PCIe Root Complex; PCS = PCIe Switch)

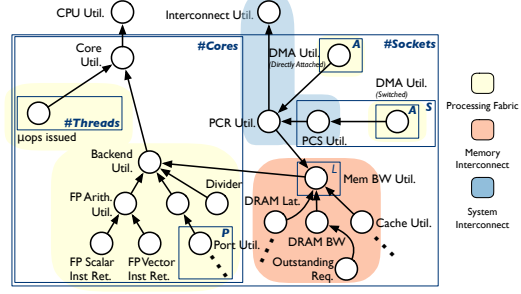


Figure 4: Bayesian network (uses Plate notation) used to estimate resource utilization.

sampling N times between successive scheduler invocations to get around some of the sources of error. To maximize the performance estimation fidelity, we apply statistical methods to systematically model the variance of these measurements. For a single performance counter $o_t[c]$, if the error in measurement e_c can be modeled, then the measured value m_c can be modeled in terms of the true value v_c plus measurement noise e_c , i.e., $m_c = v_c + e_c$. Here, we focus only on random errors, by assuming zero systematic error. This is a valid assumption because the only reason for systematic errors will be hardware or software bugs. We assume that the error can be modeled as $e_c \sim \mathcal{N}(0, \sigma)$ for some unknown variance σ , hence $\Pr(m_c | v_c) = \mathcal{N}(m_c, \sigma)$ [43]. Now given N measurements of the value of the performance counter, we compute their sample mean μ and sample variance S . A scaled and shifted t-distribution describes the marginal distribution of the unknown mean of a Gaussian, when the dependence on variance has been marginalised out [44], i.e.,

$$v_c \sim \mu + S/\sqrt{N} \text{ Student}(\nu = N - 1). \quad (6)$$

In all our experiments, the confidence level of the t-distribution is set to 95%.

Now, given a distribution of v_c for every element of o_t , we describe the construction of the BN model. Our goal is to model resource utilization (a number in $[0, 1]$) for a relevant set of architectural resources R . To do this, we use algebraic models of composing PC measurements (v_c) using algebraic (deterministic) based on information about the CPU architecture. Processor performance manuals [45–47] provide this information. Given that our error corrected measurements are defined in terms of distributions, the algebraic models that encode static information about relationships (based on the microarchitecture of the processor or topology of the system) now define statistical relationships $v_{c,s}$ (based on the Jacobian relationships described in §3). Fig. 4 shows an example of the BN model. However, the types and meanings of hardware counters vary from one kind of architecture to another due to the variation in hardware organizations. As a result, the model defined by the BN is parametric, changing with different processors and system topologies (i.e., across all the different types of systems in a datacenter). Consider the example of identifying memory bandwidth utilization for a CPU core. According to the processor documentation this utilization can be computed by measuring the number of outstanding memory requests (which is available as a PC), i.e., $\text{Outstanding Requests}[\geq \theta_{MB}] / \text{Outstanding Requests}[\geq 1]$. The notation $X[\geq t]$ counts cycles in which X exceed threshold t . The value θ_{MB} is processor specific and might not always be known. In such cases, we use the training approach described in §3 to learn θ_{MB} . We follow a similar procedure to estimate the other utilization of other resources in the system, these are labeled “Util.” in Fig. 4.

NN Model. The second part of the proposed POMDP based scheduling model uses a NN (see Fig. 2) to learn the optimal policy to schedule user tasks given a belief state. This NN takes two graphs as inputs. The first input, is the belief state \hat{b}_t encoded as vertex labels on a graph describing the topology of a computer system (i.e., the organization shown in Fig. 3), and input labels corresponding to locations of inputs in the topology. The second input is the user’s program expressed as a DFG. We use *graph network* (GN) layers [48] to “embed” these graphs into a set of *embedding vectors*. GNs have been shown to capture node, edge, and locality information. We choose small fully connected NNs to model the functional transformations in the GN layers. Prior work in scheduling (e.g., [49, 50]) has shown benefit of considering temporal information to capture dependencies of system resources over time, as well capture time evolution of the user DFG. We capture these relationships (between the embeddings of the input graphs) using a RNN, particularly an LSTM layer [51].

The action space \mathcal{A} of the model is fixed as the number of kernels/processors available in the system is known ahead of time. The action space consists of the following types of actions. (i) *Execution*

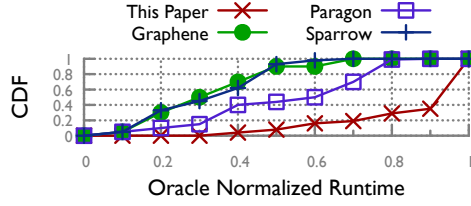


Figure 5: Comparing performance to other popular schedulers for kernel executions in DFGs.

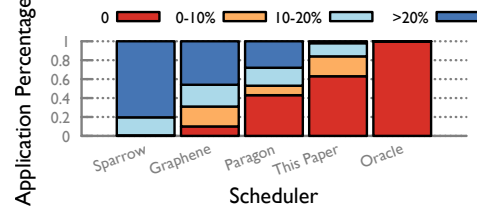


Figure 6: Percentage of application executions that shows a degradation in performance.

actions corresponding to executing a kernel on a processor/accelerator. (ii) *Reconfiguration actions* corresponding to reconfiguring a single FPGA context to a kernel. (iii) *No-Op action* corresponding to not scheduling any task in a particular scheduler invocation. This action is useful in when the system resources are maximally subscribed, and executing more tasks will hinder performance.

The reward r_t is based on the objective of minimizing the runtime of a user DFG. At time t , $r_t = -\sum_{i=0}^t 1/T_i$, where T_i is the wall clock time taken to execute the i actions executing in the system at time t . Note that parallel actions are not double-counted in this formulation. The BN and NN models are trained end-to-end using minimization of Eqn. (1) through backpropagation as described in §3. Implementation details are presented in the supplementary material.

5 Evaluation & Discussion

We evaluate the proposed scheduling model and training technique along the following dimensions. (i) *How well does the scheduler perform compared to the state of the art?* (ii) *What are the savings in training time compared to traditional methods?* The evaluation testbed consists of a rack-scale cluster of twelve IBM Power8 CPUs, two NVIDIA K40, six K80 GPUs, and two FPGAs. We illustrate the generality of techniques on a variety of real-world workloads that use CPUs, GPUs and FPGAs: (i) *variant calling and genotyping analysis* [52] on human genome datasets appropriate for clinical use (using tools presented in [53–58, 38, 59–61, 59, 62–64]), (ii) *epilepsy detection and localization* [65, 66] on intra-cranial electroencephalography data; (iii) in online *security analytics* [67, 66] on network- and host-level intrusion detection system event-streams.

State of the Art. Traditional dynamic scheduling techniques (e.g., [5–10]) use manually tuned heuristics (e.g., fairness, shortest-job-first) that prioritize simplicity and generality over achieving the best-case workload performance. The complexity (NP-Hard) of the job shop scheduling problem limits these techniques to use these approximate heuristics, allocate coarse grained resources (e.g., GBs of memory, CPU threads) and make simplifying homogeneity assumptions about the underlying processors (i.e., all processors are same). Several ML-based scheduling strategies have also been proposed, where the above heuristics are learned from data. These range from those that make simplifying assumptions about the workload and processing fabric (e.g., [68, 69]) to those that treat system as black-boxes to perform scheduling to optimize processor-specific throughput metrics (e.g., [11–17]). In fact, deep RL has been applied in cluster scheduling in [68, 69], however, those works assume a completely model-free NN using only the aspects of the system state that can be measured directly. These approaches are not suited for heterogeneous accelerator-rich systems where architectural diversity necessitates the use low-level resources, which cannot be measured directly, and are not semantically comparable across processors. As points of comparison to the method proposed here we use *Graphene* [49], a heuristic-accelerated job shop optimization solver, *Sparrow* [8], a randomized scheduler, and *Paragon* [14], a collaborative filtering based scheduler.¹

Baseline for Comparison. We define the *oracle schedule* to correspond to the best performance possible for running an application on the evaluation system. This corresponds to a completely isolated execution of an application. Here different concurrently executing kernels of the same application contend for resources and might cause performance degradation. For the benchmark applications, we have accounted for this by exhaustively executing schedules of the application DFGs to find the one with the lowest runtime. Corresponding to this execution, we measure the runtime of kernel i in workload (DFG) j as $t_{i,j}^{\text{oracle}}$ across all kernels and workloads. $t_{i,j}^{\text{oracle}}$ serves as the baseline for comparison of the performance of the proposed scheduler.

¹The Pulsar implementation uses application throughput as the performance metric. We provide of 50% all possible combinations of processors and kernels performance (i.e., sparsity of the collaborative filtering matrix).

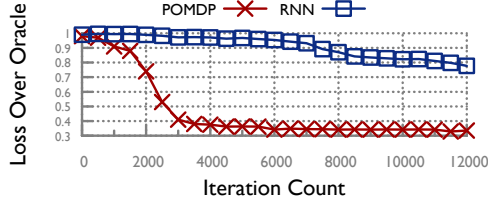


Figure 7: Sample efficiency of the POMDP. An iteration consists of 2 RL episodes of 20 steps.

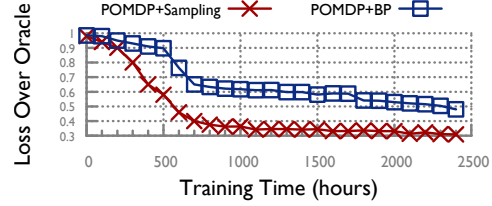


Figure 8: Effectiveness of sampling strategy over Bayesian inference.

Effectiveness of Scheduling Model. First, we quantify how well the proposed model can handle scheduling of kernels in a DFG considering interference both the intra DFG level when executing with an unknown co-located workload utilizing compute and I/O resources. To do so, we measure the runtimes of each of the kernels i in the workload j (as above) to compute $t_{i,j}^s$ for each scheduler s under test. In Fig. 5, we illustrate the distribution of oracle normalized runtimes for each of the kernels in the workloads we are testing, i.e., distribution of $t_{i,j}^s/t_{i,j}^{\text{oracle}}$ across 500 executions of the three above workloads. In the figure, a distribution with probability mass is closest to 1 is preferred, as it implies the least slowdown over the oracle. We observe that the proposed technique significantly outperforms the state of the art: the median and at the 99th-percentile of all executions the proposed technique outperforms the second closest (in this case Paragon) by close to 32%. At the 99th-percentile, the generated schedules perform at 6% loss over the the oracle. Next, we quantify the performance of end-to-end user workloads in Fig. 6. Here we calculate $1 - (\sum_i t_{i,j}^s)/(\sum_i t_{i,j}^{\text{oracle}})$ for all 500 runs of the DFGs and group them into buckets of normalized performance. The proposed technique significantly outperforms the other scheduling techniques running as much 60% of the applications with no performance loss over the oracle execution, and the remaining with less than 20% performance loss.

Training Time. Finally we quantify the improvement in training time of the proposed model based on sampling based gradient computation methodology presented in §3. We use two baselines for evaluation: (i) using an RNN without the inductive bias of the POMDP model; and (ii) using the POMDP model, but with traditional gradient based training where full Bayesian inference is calculated using belief propagation (BP). The RNN model here, replaces the BN (and inference) and system topology embedding GN (in Fig. 2) with a 3-layer fully connected NN to compute an embedding for o_t . Fig. 7 illustrates the difference in performance of the three configurations when considering loss in performance of the user DFGs over the oracle schedule (i.e., $1 - (\sum_i t_{i,j}^s)/(\sum_i t_{i,j}^{\text{oracle}})$). We observe that the RNN is significantly less sample efficient than the proposed POMDP: using a linear extrapolation (which is very optimistic) from iteration 12k, the RNN would need 48k+ more iterations to reach the same accuracy as the POMDP.

Now, the scheduler configurations “POMDP+BP” and “POMDP+Sampling” (i.e., gradient computation proposed in this paper) are equally efficient when it comes to sampling trajectories, they differ in time taken to perform backpropagation based parameter updates. Fig. 8 illustrates the approximately $4\times$ difference in this training time between the two configurations, for the model to reach 30% mean loss over the oracle. This reduction is significant because the continuous churn of user workloads and machine configurations in a cloud [11] would require periodically retraining the scheduling model. In absolute terms, the “POMDP+Sampling” configuration is able to achieve 30% loss over the oracle schedule in 700 hours of training (from Fig. 8) and ~ 3700 iterations of workload execution (from Fig. 8), which corresponds to approximately 500 hours of system execution, hence the total process takes 1200 hours. Though this might appear to be over 7 weeks of time, in wall clock time this is approximately 2 week because we use parallel A3C-based training. In fact, the limiting factor here is the availability of FPGAs, of which we have only 2 in the evaluation cluster, hence limiting the number of RL episodes that can be run in parallel.

6 Conclusion

This paper presents an RL-agent that integrates domain knowledge to schedule DFGs across heterogeneous processors. The key novelty of our approach is (i) the RL model; and (ii) the significant reduction of training-data (using domain knowledge) and -time (using sampling based end-to-end gradient propagation). With datacenter architectures become complex [2, 1], techniques like the one proposed here will be fundamental in deploying future accelerated applications.

References

- [1] K. Asanovic and D. Patterson. Firebox: A hardware building block for 2020 warehouse-scale computers. In *USENIX FAST*, volume 13, 2014.
- [2] Y. Shao and D. Brooks. *Research Infrastructures for Hardware Accelerators*. Synthesis Lectures on Computer Architecture. Morgan & Claypool Publishers, 2015.
- [3] M. Mastrolilli and O. Svensson. (acyclic) job shops are hard to approximate. In *2008 49th Annual IEEE Symposium on Foundations of Computer Science*, pages 583–592, Oct 2008.
- [4] M. Mastrolilli and O. Svensson. Improved bounds for flow shop scheduling. In *International Colloquium on Automata, Languages, and Programming*, pages 677–688. Springer, 2009.
- [5] M. Isard, V. Prabhakaran, J. Currey, U. Wieder, K. Talwar, and A. Goldberg. Quincy: Fair scheduling for distributed computing clusters. In *Proceedings of the ACM SIGOPS 22Nd Symposium on Operating Systems Principles, SOSP '09*, pages 261–276, New York, NY, USA, 2009. ACM.
- [6] S. Zhuravlev, S. Blagodurov, and A. Fedorova. Addressing shared resource contention in multicore processors via scheduling. *SIGPLAN Not.*, 45(3):129–142, March 2010.
- [7] M. Zaharia, D. Borthakur, J. Sen Sarma, K. Elmeleegy, S. Shenker, and I. Stoica. Delay scheduling: A simple technique for achieving locality and fairness in cluster scheduling. In *Proceedings of the 5th European Conference on Computer Systems, EuroSys '10*, pages 265–278, New York, NY, USA, 2010. ACM.
- [8] K. Ousterhout, P. Wendell, M. Zaharia, and I. Stoica. Sparrow: Distributed, low latency scheduling. In *Proceedings of the Twenty-Fourth ACM Symposium on Operating Systems Principles, SOSP '13*, pages 69–84, New York, NY, USA, 2013. ACM.
- [9] J. Giceva, G. Alonso, T. Roscoe, and T. Harris. Deployment of query plans on multicores. *Proc. VLDB Endow.*, 8(3):233–244, November 2014.
- [10] R. Lyerly, A. Murray, A. Barbalace, and B. Ravindran. Aira: A framework for flexible compute kernel execution in heterogeneous platforms. *IEEE Transactions on Parallel and Distributed Systems*, 29(2):269–282, Feb 2018.
- [11] J. Mars, L. Tang, and R. Hundt. Heterogeneity in “homogeneous” warehouse-scale computers: A performance opportunity. *IEEE Comput. Archit. Lett.*, 10(2):29–32, July 2011.
- [12] J. Mars and L. Tang. Whare-map: Heterogeneity in “homogeneous” warehouse-scale computers. *SIGARCH Comput. Archit. News*, 41(3):619–630, June 2013.
- [13] H. Yang, A. Breslow, J. Mars, and L. Tang. Bubble-flux: Precise online qos management for increased utilization in warehouse scale computers. In *Proceedings of the 40th Annual International Symposium on Computer Architecture, ISCA '13*, pages 607–618, New York, NY, USA, 2013. ACM.
- [14] C. Delimitrou and C. Kozyrakis. Paragon: Qos-aware scheduling for heterogeneous datacenters. *SIGPLAN Not.*, 48(4):77–88, March 2013.
- [15] C. Delimitrou and C. Kozyrakis. Quasar: Resource-efficient and qos-aware cluster management. In *Proceedings of the 19th International Conference on Architectural Support for Programming Languages and Operating Systems, ASPLOS '14*, pages 127–144, New York, NY, USA, 2014. ACM.
- [16] Y. Zhang, M. A. Laurenzano, J. Mars, and L. Tang. Smite: Precise qos prediction on real-system smt processors to improve utilization in warehouse scale computers. In *2014 47th Annual IEEE/ACM International Symposium on Microarchitecture*, pages 406–418, Dec 2014.
- [17] L. Xu, A. R. Butt, S. Lim, and R. Kannan. A heterogeneity-aware task scheduler for spark. In *2018 IEEE International Conference on Cluster Computing (CLUSTER)*, pages 245–256, Sep. 2018.

- [18] K. J. Astrom. Optimal control of markov processes with incomplete state information. *Journal of mathematical analysis and applications*, 10(1):174–205, 1965.
- [19] L. P. Kaelbling, M. L. Littman, and A. R. Cassandra. Planning and acting in partially observable stochastic domains. *Artificial intelligence*, 101(1-2):99–134, 1998.
- [20] V. Mnih, A. P. Badia, M. Mirza, A. Graves, T. Harley, T. P. Lillicrap, D. Silver, and K. Kavukcuoglu. Asynchronous methods for deep reinforcement learning. In *Proceedings of the 33rd International Conference on International Conference on Machine Learning - Volume 48*, ICML’16, pages 1928–1937. JMLR.org, 2016.
- [21] P. Dhariwal, C. Hesse, O. Klimov, A. Nichol, M. Plappert, A. Radford, J. Schulman, S. Sidor, Y. Wu, and P. Zhokhov. Openai baselines. *GitHub, GitHub repository*, 2017.
- [22] R. S. Dreyer and D. B. Alpert. Apparatus for monitoring the performance of a microprocessor, August 12 1997. US Patent 5,657,253.
- [23] P. Dagum and M. Luby. Approximating probabilistic inference in bayesian belief networks is np-hard. *Artificial Intelligence*, 60(1):141 – 153, 1993.
- [24] S. Russell, J. Binder, D. Koller, and K. Kanazawa. Local learning in probabilistic networks with hidden variables. In *Proceedings of the 14th International Joint Conference on Artificial Intelligence - Volume 2*, IJCAI’95, pages 1146–1152, San Francisco, CA, USA, 1995. Morgan Kaufmann Publishers Inc.
- [25] J. Binder, D. Koller, S. Russell, and K. Kanazawa. Adaptive probabilistic networks with hidden variables. *Machine Learning*, 29(2/3):213–244, 1997.
- [26] M. Hausknecht and P. Stone. Deep recurrent q-learning for partially observable mdps. In *2015 AAAI Fall Symposium Series*, 2015.
- [27] K. Narasimhan, T. Kulkarni, and R. Barzilay. Language understanding for text-based games using deep reinforcement learning. *arXiv preprint arXiv:1506.08941*, 2015.
- [28] V. Mnih, K. Kavukcuoglu, D. Silver, A. A. Rusu, J. Veness, M. G. Bellemare, A. Graves, M. Riedmiller, A. K. Fidjeland, G. Ostrovski, et al. Human-level control through deep reinforcement learning. *Nature*, 518(7540):529, 2015.
- [29] M. Jaderberg, V. Mnih, W. M. Czarnecki, T. Schaul, J. Z. Leibo, D. Silver, and K. Kavukcuoglu. Reinforcement learning with unsupervised auxiliary tasks. *arXiv preprint arXiv:1611.05397*, 2016.
- [30] J. N. Foerster, Y. M. Assael, N. de Freitas, and S. Whiteson. Learning to communicate to solve riddles with deep distributed recurrent q-networks. *arXiv preprint arXiv:1602.02672*, 2016.
- [31] P. Karkus, D. Hsu, and W. S. Lee. Qmdp-net: Deep learning for planning under partial observability. In *Advances in Neural Information Processing Systems*, pages 4694–4704, 2017.
- [32] P. Zhu, X. Li, P. Poupart, and G. Miao. On improving deep reinforcement learning for pomdps. *arXiv preprint arXiv:1804.06309*, 2018.
- [33] D. Silver, H. van Hasselt, M. Hessel, T. Schaul, A. Guez, T. Harley, G. Dulac-Arnold, D. Reichert, N. Rabinowitz, A. Barreto, et al. The predictron: End-to-end learning and planning. In *Proceedings of the 34th International Conference on Machine Learning-Volume 70*, pages 3191–3199. JMLR. org, 2017.
- [34] M. Igl, L. Zintgraf, T. A. Le, F. Wood, and S. Whiteson. Deep variational reinforcement learning for pomdps. *arXiv preprint arXiv:1806.02426*, 2018.
- [35] V. R. Konda and J. N. Tsitsiklis. Actor-critic algorithms. In *Advances in neural information processing systems*, pages 1008–1014, 2000.
- [36] R. D. Shachter. Bayes-ball: The rational pastime (for determining irrelevance and requisite information in belief networks and influence diagrams). *arXiv preprint arXiv:1301.7412*, 2013.

- [37] K. Asanovic, R. Bodik, J. Demmel, T. Keaveny, K. Keutzer, J. Kubiawicz, N. Morgan, D. Patterson, K. Sen, J. Wawrzynek, D. Wessel, and K. Yelick. A view of the parallel computing landscape. *Commun. ACM*, 52(10):56–67, October 2009.
- [38] S. S. Banerjee, A. P. Athreya, L. S. Mainzer, C. V. Jongeneel, W.-M. Hwu, Z. T. Kalbarczyk, and R. K. Iyer. Efficient and scalable workflows for genomic analyses. In *Proceedings of the ACM International Workshop on Data-Intensive Distributed Computing, DDC ’16*, pages 27–36, New York, NY, USA, 2016. ACM.
- [39] M. Abadi, P. Barham, J. Chen, Z. Chen, A. Davis, J. Dean, M. Devin, S. Ghemawat, G. Irving, M. Isard, M. Kudlur, J. Levenberg, R. Monga, S. Moore, D. G. Murray, B. Steiner, P. Tucker, V. Vasudevan, P. Warden, M. Wicke, Y. Yu, and X. Zheng. Tensorflow: A system for large-scale machine learning. In *Proceedings of the 12th USENIX Conference on Operating Systems Design and Implementation, OSDI’16*, pages 265–283, Berkeley, CA, USA, 2016. USENIX Association.
- [40] C. Chambers, A. Raniwala, F. Perry, S. Adams, R. Henry, R. Bradshaw, and Nathan. Flumejava: Easy, efficient data-parallel pipelines. In *ACM SIGPLAN Conference on Programming Language Design and Implementation (PLDI)*, pages 363–375, 2 Penn Plaza, Suite 701 New York, NY 10121-0701, 2010.
- [41] M. Zaharia, M. Chowdhury, T. Das, A. Dave, J. Ma, M. McCauley, M. J. Franklin, S. Shenker, and I. Stoica. Resilient distributed datasets: A fault-tolerant abstraction for in-memory cluster computing. In *Proceedings of the 9th USENIX Conference on Networked Systems Design and Implementation, NSDI’12*, pages 2–2, Berkeley, CA, USA, 2012. USENIX Association.
- [42] M. McCool, J. Reinders, and A. Robison. *Structured Parallel Programming: Patterns for Efficient Computation*. Morgan Kaufmann Publishers Inc., San Francisco, CA, USA, 1st edition, 2012.
- [43] V. M. Weaver and S. A. McKee. Can hardware performance counters be trusted? In *2008 IEEE International Symposium on Workload Characterization*, pages 141–150. IEEE, 2008.
- [44] A. Gelman, J. Carlin, H. Stern, and D. Rubin. *Bayesian Data Analysis*. Chapman & Hall, New York, 1995.
- [45] A. Yasin. A top-down method for performance analysis and counters architecture. In *2014 IEEE International Symposium on Performance Analysis of Systems and Software (ISPASS)*, pages 35–44, March 2014.
- [46] I. Corp. Intel® 64 and IA-32 Architectures Software Developer Manuals. <https://software.intel.com/en-us/articles/intel-sdm>, 2016. Accessed 2019-03-05.
- [47] B. Hall, P. Bergner, A. S. Housfater, M. Kandasamy, T. Magno, A. Mericas, S. Munroe, M. Oliveira, B. Schmidt, W. Schmidt, et al. *Performance optimization and tuning techniques for IBM Power Systems processors including IBM POWER8*. IBM Redbooks, 2017.
- [48] P. W. Battaglia, J. B. Hamrick, V. Bapst, A. Sanchez-Gonzalez, V. Zambaldi, M. Malinowski, A. Tacchetti, D. Raposo, A. Santoro, R. Faulkner, et al. Relational inductive biases, deep learning, and graph networks. *arXiv preprint arXiv:1806.01261*, 2018.
- [49] R. Grandl, S. Kandula, S. Rao, A. Akella, and J. Kulkarni. Graphene: Packing and dependency-aware scheduling for data-parallel clusters. In *Proceedings of the 12th USENIX Conference on Operating Systems Design and Implementation, OSDI’16*, pages 81–97, Berkeley, CA, USA, 2016. USENIX Association.
- [50] H. Wu, G. Diamos, S. Cadambi, and S. Yalamanchili. Kernel weaver: Automatically fusing database primitives for efficient gpu computation. In *2012 45th Annual IEEE/ACM International Symposium on Microarchitecture*, pages 107–118, Dec 2012.
- [51] S. Hochreiter and J. Schmidhuber. Long short-term memory. *Neural computation*, 9(8):1735–1780, 1997.

- [52] G. A. Van der Auwera, M. O. Carneiro, C. Hartl, R. Poplin, G. del Angel, A. Levy-Moonshine, T. Jordan, K. Shakir, D. Roazen, J. Thibault, E. Banks, K. V. Garimella, D. Altshuler, S. Gabriel, and M. A. DePristo. *From FastQ Data to High-Confidence Variant Calls: The Genome Analysis Toolkit Best Practices Pipeline*. John Wiley & Sons, Inc., 2013.
- [53] H. Li and R. Durbin. Fast and accurate short-read alignment with burrows-wheeler transform. *Bioinformatics*, 25(14):1754–1760, may 2009.
- [54] H. Li and R. Durbin. Fast and accurate long-read alignment with Burrows–Wheeler transform. *Bioinformatics*, 26(5):589–595, 2010.
- [55] B. Langmead, C. Trapnell, M. Pop, and S. L. Salzberg. Ultrafast and memory-efficient alignment of short DNA sequences to the human genome. *Genome Biol*, 10(3):R25, 2009.
- [56] M. Zaharia, W. J. Bolosky, K. Curtis, A. Fox, D. Patterson, S. Shenker, I. Stoica, R. M. Karp, and T. Sittler. Faster and more accurate sequence alignment with SNAP. *arXiv preprint arXiv:1111.5572*, 2011.
- [57] S. S. Banerjee, M. El-Hadedy, J. B. Lim, Z. T. Kalbarczyk, D. Chen, S. S. Lumetta, and R. K. Iyer. Asap: Accelerated short-read alignment on programmable hardware. *IEEE Transactions on Computers*, 68(3):331–346, March 2019.
- [58] S. S. Banerjee, M. El-Hadedy, J. B. Lim, D. Chen, Z. T. Kalbarczyk, D. Chen, and R. K. Iyer. ASAP: accelerated short read alignment on programmable hardware (abstract only). In *Proceedings of the 2017 ACM/SIGDA International Symposium on Field-Programmable Gate Arrays, FPGA 2017, Monterey, CA, USA, February 22-24, 2017*, pages 293–294, 2017.
- [59] A. McKenna, M. Hanna, E. Banks, A. Sivachenko, K. Cibulskis, A. Kernysky, K. Garimella, D. Altshuler, S. Gabriel, M. Daly, and M. A. DePristo. The genome analysis toolkit: A MapReduce framework for analyzing next-generation DNA sequencing data. *Genome Research*, 20(9):1297–1303, jul 2010.
- [60] F. A. Nothaft, M. Massie, T. Danford, Z. Zhang, U. Laserson, C. Yeksigian, J. Kottalam, A. Ahuja, J. Hammerbacher, M. Linderman, M. J. Franklin, A. D. Joseph, and D. A. Patterson. Rethinking data-intensive science using scalable analytics systems. In *Proceedings of the 2015 ACM SIGMOD International Conference on Management of Data, SIGMOD ’15*, pages 631–646, New York, NY, USA, 2015. ACM.
- [61] H. Li, B. Handsaker, A. Wysoker, T. Fennell, J. Ruan, N. Homer, G. Marth, G. Abecasis, R. Durbin, et al. The sequence alignment/map format and SAMtools. *Bioinformatics*, 25(16):2078–2079, 2009.
- [62] F. Nothaft. Scalable genome resequencing with adam and avocado. Master’s thesis, EECS Department, University of California, Berkeley, May 2015.
- [63] A. Rimmer, H. Phan, I. Mathieson, Z. Iqbal, S. R. F. Twigg, A. O. M. Wilkie, G. McVean, and G. Lunter. Integrating mapping-, assembly- and haplotype-based approaches for calling variants in clinical sequencing applications. *Nature Genetics*, 46(8):912–918, jul 2014.
- [64] S. S. Banerjee, M. El-Hadedy, C. Y. Tan, Z. T. Kalbarczyk, S. S. Lumetta, and R. K. Iyer. On accelerating pair-hmm computations in programmable hardware. In *27th International Conference on Field Programmable Logic and Applications, FPL 2017, Ghent, Belgium, September 4-8, 2017*, pages 1–8, 2017.
- [65] Y. Varatharajah, M. J. Chong, K. Saboo, B. Berry, B. Brinkmann, G. Worrell, and R. Iyer. Eeg-graph: A factor-graph-based model for capturing spatial, temporal, and observational relationships in electroencephalograms. In *Advances in Neural Information Processing Systems*, pages 5377–5386, 2017.
- [66] S. S. Banerjee, Z. T. Kalbarczyk, and R. K. Iyer. Acmc 2 : Accelerating markov chain monte carlo algorithms for probabilistic models. In *Proceedings of the Twenty-Fourth International Conference on Architectural Support for Programming Languages and Operating Systems, ASPLOS ’19*, pages 515–528, New York, NY, USA, 2019. ACM.

- [67] P. Cao, E. Badger, Z. Kalbarczyk, R. Iyer, and A. Slagell. Preemptive intrusion detection: Theoretical framework and real-world measurements. In *Proceedings of the 2015 Symposium and Bootcamp on the Science of Security, HotSoS '15*, pages 5:1–5:12, New York, NY, USA, 2015. ACM.
- [68] H. Mao, M. Alizadeh, I. Menache, and S. Kandula. Resource management with deep reinforcement learning. In *Proceedings of the 15th ACM Workshop on Hot Topics in Networks*, pages 50–56. ACM, 2016.
- [69] H. Mao, M. Schwarzkopf, S. B. Venkatakrisnan, Z. Meng, and M. Alizadeh. Learning scheduling algorithms for data processing clusters. *arXiv preprint arXiv:1810.01963*, 2018.